



Available online at www.sciencedirect.com

ScienceDirect

Geochimica et Cosmochimica Acta 261 (2019) 383–395

Geochimica et Cosmochimica Acta

www.elsevier.com/locate/gca

CO₂-dependent carbon isotope fractionation in Archaea, Part II: The marine water column

Sarah J. Hurley ^{a,b,*}, Hilary G. Close ^c, Felix J. Elling ^a, Claire E. Jasper ^a, Kalina Gospodinova ^d, Ann P. McNichol ^d, Ann Pearson ^{a,*}

^a Department of Earth and Planetary Sciences, Harvard University, Cambridge, MA 02138, USA
^b Department of Geological Sciences, University of Colorado Boulder, Boulder, CO 80309, USA
^c Rosenstiel School of Marine and Atmospheric Science, University of Miami, Miami, FL 33149, USA
^d Woods Hole Oceanographic Institution, Woods Hole, MA 02543, USA

Received 25 December 2018; accepted in revised form 21 June 2019; Available online 2 July 2019

Abstract

Stable carbon isotope ratios of archaeal glycerol dibiphytanyl glycerol tetraether (GDGT) lipids have been proposed as a proxy to infer past changes in the carbon isotope composition ($\delta^{\bar{1}3}$ C) of dissolved inorganic carbon (DIC). The premise for paleo- $\delta^{13}C_{DIC}$ reconstructions from GDGTs is based on observations of relatively constant $\delta^{13}C_{GDGT}$ values in recent depositional environments. Marine Thaumarchaeota, thought to be the dominant source of GDGTs to marine sediments, fix inorganic carbon using the 3-hydroxypropionate/4-hydroxybutyrate (3HP/4HB) pathway, which is specific to HCO₃ as the substrate. Bicarbonate-dependent autotrophy has been the basis for predicting that the stable carbon isotopic composition of GDGTs ($\delta^{13}C_{GDGT}$) should vary in parallel with water column $\delta^{13}C_{DIC}$ values, because HCO $_{3}$ is by far the dominant fraction of DIC in modern seawater. However, this relationship has never been systematically tested. Here we examine the carbon isotopic composition of GDGTs from four water column profiles in the Southwest and Equatorial Atlantic Ocean. Values of $\delta^{13}C_{GDGT}$ increase with depth in the water column, in contrast to the characteristic decrease in $\delta^{13}C_{DIC}$ values. These divergent trends imply a decrease in the observed total biosynthetic isotope effect (ε_{Ar}) with depth, i.e., the offset between $\delta^{13}C_{DIC}$ and $\delta^{13}C_{GDGT}$ is not constant. Instead, we find that values of ε_{Ar} specifically correlate with oceanographic variables associated with extent of organic remineralization, decreasing as CO₂ concentration increases. This observed relationship is consistent in both magnitude and direction with the results of an isotope flux-balance model for Thaumarchaeota that suggests ε_{Ar} should be sensitive to growth rate (μ) and CO₂ availability under conditions of atmospheric pCO₂ < 4 times the pre-anthropogenic Holocene level. Further tests of the sensitivity of ε_{Ar} to μ and CO₂ in the modern marine environment will be essential to exploring the potential for a new, archaeal lipid-derived pCO₂ paleobarometer. © 2019 Elsevier Ltd. All rights reserved.

Keywords: Archaea; Stable carbon isotopes; PCO2 proxy; GDGTs; Biomarkers

E-mail addresses: sarah.hurley@colorado.edu (S.J. Hurley), pearson@eps.harvard.edu (A. Pearson).

1. INTRODUCTION

Glycerol dibiphytanyl glycerol tetraether (GDGT) lipids of archaeal membranes are preserved in marine sediments from the Jurassic to the present (e.g., Jenkyns et al., 2012). These biomarkers record the presence and activity of marine planktonic archaea, which are ubiquitous in the

^{*} Corresponding authors at: Department of Earth and Planetary Sciences, Harvard University, Cambridge, MA 02138, USA (S.J. Hurley).

marine water column (Fuhrman et al., 1992; DeLong, 1992; Karner et al., 2001) and form the basis of the TEX₈₆ pale-otemperature proxy (Schouten et al., 2002).

The dominant source of GDGTs to sediments generally is believed to be the marine group I.1a Thaumarchaeota (e.g., Pearson and Ingalls, 2013). These archaea oxidize ammonia and fix carbon autotrophically using the 3-hydro xypropionate/4-hydroxybutyrate pathway (3HP/4HB) (Könneke et al., 2005; Berg et al., 2007; Könneke et al., 2014). Thaumarchaeota are most abundant and active near the base of the euphotic zone (Francis et al., 2005; Beman et al., 2008; Church et al., 2010; Santoro et al., 2010). Marine group II Euryarchaeota also are common, primarily in surface waters (Massana et al., 1997; Massana et al., 1998; Massana et al., 2000). Their presumed heterotrophic metabolism has largely been inferred from metagenomics due to a lack of cultured representatives (Frigaard et al., 2006; Iverson et al., 2012; Martin-Cuadrado et al., 2014; Orsi et al., 2015; Santoro et al., 2019). Recently Lincoln et al. (2014) proposed that these Euryarchaeota may also contribute to the GDGT pool, although this remains debated (Schouten et al., 2014), and to date only Thaumarchaeota are known to produce the distinctive cyclohexane ringcontaining GDGT, crenarchaeol (Elling et al., 2017).

Due to the presumed dominance of total planktonic archaeal production by autotrophic Thaumarchaeota, stable carbon isotope measurements of GDGTs have been proposed as a tool to infer past changes in marine $\delta^{13}C_{DIC}$ values (Hoefs et al., 1997; Schouten et al., 1998), for example during Cretaceous ocean anoxic events (Kuypers et al., 2001) or other episodes where carbonate sedimentation is restricted or absent. However, the fidelity of a proposed paleo- $\delta^{13}C_{DIC}$ proxy requires that carbon assimilation by Thaumarchaeota be accompanied by a constant biosynthetic isotope effect (ϵ_{Ar} , signifying the difference between the inorganic carbon source and the archaeal biomass), and that there be minimal influence from mixotrophic or heterotrophic carbon assimilation, including any contributions by Euryarchaeota.

To date, preliminary evidence that GDGTs could serve as a paleo- $\delta^{13}C_{DIC}$ proxy has invoked the relatively constant $\delta^{13}C$ value of $-21\pm1.5\%$ for the crenarchaeolspecific $C_{40:3}$ biphytane (sidechain hydrocarbon) observed in recent depositional environments (Schouten et al., 2013). The 3HP/4HB pathway of carbon fixation in Thaumarchaeota is specific to HCO_3^- , leading to the supposition that a relatively stable ocean $\delta^{13}C_{DIC}$ signature (mostly reflecting $\delta^{13}C_{HCO3-}$ values), high and relatively invariant [HCO $_3^-$], and a constant biosynthetic ϵ_{Ar} value would lead to stable values of $\delta^{13}C_{GDGT}$ for the entire exported pool of water-column GDGTs.

However, a limited survey of recent core-top sediments showed that $\delta^{13}C_{GDGT}$ values, including the Thaumarchaeota-specific crenarchaeol, are not truly constant with respect to $\delta^{13}C_{DIC}$ values (Pearson et al., 2016). This finding, plus earlier carbon isotopic measurements (Ingalls et al., 2006), were interpreted as reflecting a small but significant (~20%) contribution of heterotrophically-assimilated organic carbon by the total archaeal community. Although marine Thaumarchaeota take up amino

acids (Ouverney and Fuhrman, 2000; Teira et al., 2004; Herndl et al., 2005; Qin et al., 2014), and some strains of soil-group I.1b Thaumarchaeota appear to require pyruvate supplementation (Tourna et al., 2011), recent work has proposed that the role for organic acids is to detoxify oxygen radicals formed as a byproduct of ammonia oxidation (Kim et al., 2016). Organic carbon does not appear to be incorporated into biomass, nor do organic substrates actually promote growth (Kim et al., 2016). This would suggest that lipid isotope studies may have overestimated the contribution of mixotrophy or heterotrophy to Thaumarchaeota, and that other factors should be considered in the interpretation of non-constant $\delta^{13}C_{GDGT}$ values.

Here we investigated the ¹³C content of individual GDGTs previously quantified (Hurley et al., 2018) from a water-column transect in the Southwest and Equatorial Atlantic Ocean (~40°S to 10°N). Our results show that $\delta^{13}C_{GDGT}$ values vary inversely to the gradient of $\delta^{13}C_{DIC}$, and that ε_{Ar} differs both between locations and with depth. These patterns are not correlated with δ^{13} C values for particulate organic carbon (δ¹³C_{POC}) and are not well explained by heterotrophic processes. Instead, the response of ε_{Ar} is consistent with a recent model that suggests δ¹³C_{GDGT} values for Thaumarchaeota should respond to in situ pH and [CO_{2(aq)}] (Pearson et al., 2019). Although the magnitude of the CO₂-dependence is small, showing a total range of < 5% for ε_{Ar} through the water column, the consistency between the data and the model suggest that δ¹³C_{GDGT} values – specifically those measured for crenarchaeol - could be used as a pCO₂ proxy. Previouslyreported $\delta^{13}C_{GDGT}$ values from sediments are reinterpreted within this framework and highlight both the promise and limitations of the application.

2. METHODS

Our sampling and extraction approach is described in detail in Hurley et al. (2018). Briefly, samples were collected from aboard the R/V Knorr during the "DeepDOM" cruise, KN210-04, in March-May 2013 from 38.0°S 45.0° W (Station 2), 22.5°S 33.0°W (Station 7), 2.7°S 28.5°W (Station 15) and 9.7°N 55.3°W (Station 23) (Fig. 1). The deep chlorophyll maximum was found at 70 m (Station 23), 60–70 m (Station 15), 125 m (Station 7), and 50–75 m (Station 2) (Hurley et al., 2018). Suspended particulate matter samples were collected between 0 and 1000 m at each station. All nutrient and CTD data have been deposited in the Biological and Chemical Oceanography Data Management Office (BCO-DMO) (Kujawinski Longnecker, 2013). The concentration of total organic carbon was measured as non-purgeable organic carbon, i.e., the sum of both dissolved and particulate carbon. Apparent oxygen utilization was calculated by the difference between a saturated concentration of O2 and the concentration of O2 measured by an SBE43 oxygen sensor, according to Weiss (1970).

Particulate organic matter was sequentially filtered from seawater *in situ* using submersible pumps (WTS–LV 08 upright: McLane Research Laboratories, Inc), with total collected volumes between 710 and 10,5181 (mean 3,0491)

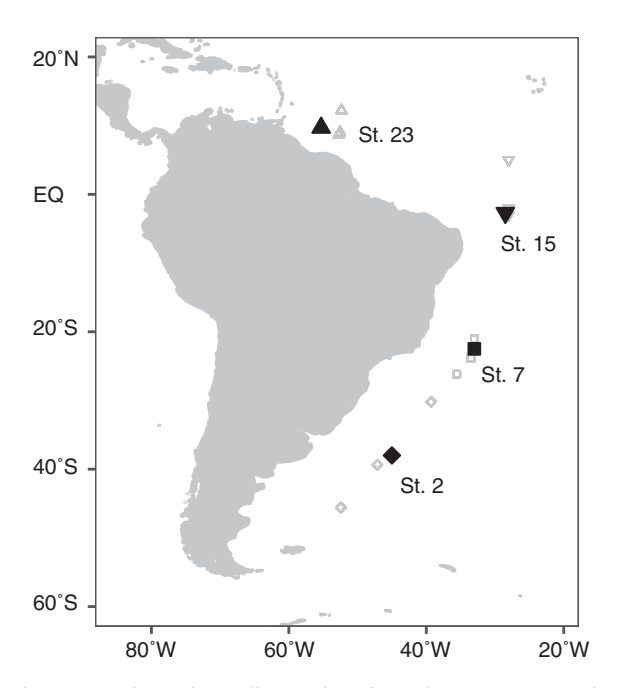


Fig. 1. Locations of sampling stations from the DeepDOM cruise (filled symbols; KN210-04 on R/V *Knorr*, March–May 2013) at 38.0°S 45.0°W (Station 2), 22.5°S 33.0°W (Station 7), 2.7°S 28.5°W (Station 15), and 9.7°N 55.3°W (Station 23). Also shown are the GLODAP station locations used to estimate CO₂ and pH profiles for each cruise station (hollow symbols).

per depth. Pumps were equipped with three filter tiers, each 142 mm in diameter. The first tier was fitted with a 53 μm mesh Nitex screen, the second with two (stacked) precombusted glass fiber filters (Whatman GF/F; 0.7 μm), and the last two (stacked) pre-combusted glass fiber filters (Sterlitech GF-75; 0.3 μm). Filters were stored in pre-combusted foil and frozen (-80 °C) immediately after collection. Values of $\delta^{13}C$ for bulk particulate organic carbon (POC) in the 0.7–53 μm size class were measured on a Europa 20–20 CF-IRMS interfaced with the Europa ANCA-SL elemental analyzer in the Stable Isotope Laboratory in The Ecosystems Center at the Marine Biological Laboratory.

Seawater samples were collected for the measurement of δ¹³C values of dissolved inorganic carbon (DIC) at the National Ocean Sciences Accelerator Mass Spectrometry (NOSAMS) facility. Pre-cleaned 500 ml stoppered Pyrex reagent bottles were supplied by NOSAMS. Bottles were rinsed and overfilled (1.5 times bottle volume), taking care to avoid bubbles, and 100 µl of saturated HgCl₂ solution was added within one minute. Ground glass joints were wiped dry and bottles were secured with pre-greased stoppers and an elastic band, shaking gently to mix poison. Values of δ^{13} C were measured using the rapid extraction of dissolved inorganic carbon from seawater (REDICS) system followed by isotopic measurement on a VG Prism isotope ratio mass spectrometer, with a demonstrated system precision of 0.04‰ (Gospodinova et al., 2015). Temperature-dependent fractionation factors from Mook et al. (1974) were then used to calculate in situ values of $\delta^{13}C_{HCO_3^-}$ from $\delta^{13}C_{DIC}$ values according to Zeebe and Wolf-Gladrow (2001). All POC and DIC isotopic data have been deposited in the Pangaea database.

Dissolved inorganic carbon (DIC) speciation was calculated according to Zeebe and Wolf-Gladrow (2001) using total DIC and pH from the Global Ocean Database Project (GLODAP; Olsen et al., 2016). We gathered water column profiles for ten locations nearest to each sampling station from the GLODAP dataset and selected the GLODAP stations with conservative properties (*i.e.*, salinity and temperature) that were most similar to the sampling stations (Fig. 1, Fig. S2) to yield consensus profiles of pH and dissolved CO₂ (Fig. 2 E, F). The error estimate for these consensus profiles corresponds to the standard deviation of the three GLODAP profiles.

2.1. Lipid extraction and separation

Filters were extracted in Teflon vessels in 90:10 CH₂Cl₂: CH₃OH using a MARS5 microwave-assisted extraction system (CEM Corporation, Matthews, NC, USA) to yield total lipid extracts (TLEs). Intact polar lipids (IPLs) and core lipids were analyzed from a 2–10% aliquot of the TLE dissolved in MeOH on a Dionex Ultimate 3000RS ultra high performance liquid chromatography (UHPLC) system connected to an ABSciEX QTRAP4500 Triple Quadrupole/Ion Trap mass spectrometry (MS) instrument equipped with a TurboIonSpray ion source operating in positive electrospray (ESI) mode as described in Hurley et al. (2018). All lipid data have been deposited in the Pangaea database under the DOI https://doi.pangaea.de/10.1594/PANGAEA.861376.

Separate aliquots of TLEs were hydrolyzed in $\sim 10~\text{ml}$ of 5% v/v HCl in MeOH for 4 h at 70 °C to yield total GDGTs for isotopic analysis. Hydrolyzed TLEs were separated over SiO2 (130–270 mesh) into three fractions: lesspolar compounds (100% hexane, followed by 25% ethyl acetate:hexane), GDGT core lipids (1:1 ethyl acetate:hexane), and polar compounds (100% ethyl acetate, followed by 100% methanol). Additional details are available in Hurley et al. (2018).

2.2. $\delta^{13}C_{GDGT}$ measurements

Individual GDGTs were purified and values of $\delta^{13}C_{GDGT}$ measured as reported previously (Ingalls et al., 2006; Shah and Pearson, 2007; Pearson et al., 2016). Briefly, the GDGT-containing fraction was purified by semi-preparative HPLC on an Agilent 1200 series HPLC equipped with a fraction collector. Normal phase HPLC (Agilent Zorbax NH₂ column, 4.6×250 mm, 5 µm particle size) was used to separate individual cyclized GDGTs, followed by reversed-phase HPLC (Agilent Zorbax Eclipse XDB-C8, 4.6×150 mm, 5 µm particle size) to remove background contaminants from each separated compound; samples were collected in fraction 2 (F2), while a leading fraction (F1) is used to assess potential contamination.

Values of $\delta^{13}C_{GDGT}$ were measured by spooling wire microcombustion–isotope ratio mass spectrometry (SWiM–IRMS; Sessions et al., 2005). The complete method

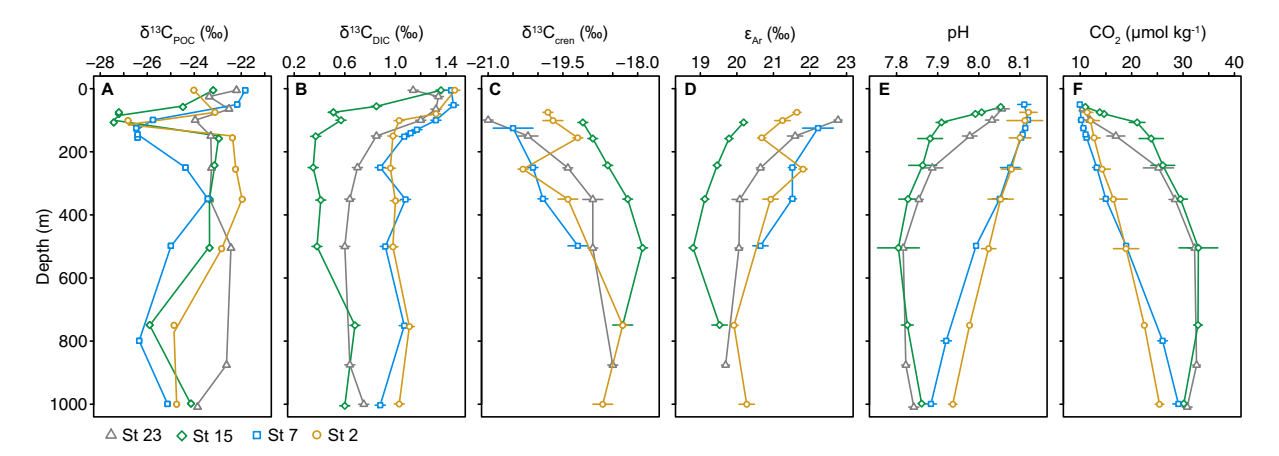


Fig. 2. Profiles of four stations in the Western Atlantic Ocean. (A) δ^{13} C values of bulk POC (0.7–53 µm size class) (B) δ^{13} C values of DIC (C) δ^{13} C values of crenarchaeol (0.7–53 µm size class) (D) ε_{Ar} values calculated according to Eq. (1) (E) averaged pH profiles. (F) Averaged CO₂ concentration profiles. Error has been propagated for all profiles; missing error bars are smaller than the data symbols. Profiles of CO₂ and pH were averaged from nearest stations in the Global Ocean Data Analysis Project (GLODAP; see supplement for evaluation of conservative properties).

is described in Pearson et al. (2016). Briefly, the fractions were dissolved in ethyl acetate and 30-100 ng were manually injected onto the wire (3 replicate injections for F1, 6 replicates for F2). The raw data were corrected for blanks and absolute offsets using dilution series of a C₄₆-GTGT standard. The 1 σ measurement precision averaged over all samples was 0.15%. Purity of the GDGT fractions was assessed using the ratio of SWiM-IRMS F2/F1 peak areas. Analysis of sedimentary F2/F1 versus δ¹³C_{GDGT} shows that F2/F1 ratios smaller than 5 may yield negatively biased δ¹³C_{GDGT} values, due to generally more negative δ13C values of the background organic matter relative to GDGTs (Pearson et al., 2016; Polik et al., 2018). However, the water column samples consistently yielded F2/F1 ratios higher than this threshold (average F2/F1 = 17 for GDGT-0; F2/F1 = 15 for minor GDGTs -1, -2, -3; and F2/F1 = 25 for crenarchaeol). All isotopic ratios are reported relative to the Vienna Pee Dee Belemnite standard. All lipid isotopic data have been deposited in the Pangaea database.

2.3. Water column model

The biosynthetic isotope effect (ϵ_{Ar}) was calculated relative to water column $HCO_3^ (H_e; \mathit{e}$ for extracellular) according to the exact formula rather than the $\epsilon_{Ar} \approx \delta^{13} C_{DIC} - \delta^{13} C_{GDGT}$ approximation:

$$\epsilon_{Ar} = 1000 \left[\frac{(\delta_{H_e})}{(\delta_{GDGT})} - 1 \right] \tag{1}$$

The error for ε_{Ar} calculations from measured *in situ* $\delta^{13}C_{HCO_3^-}$ and $\delta^{13}C_{GDGT}$ was calculated according to Freeman and Pagani (2005).

As a comparison to our observed ε_{Ar} -CO₂ relationships, the isotope flux-balance model of Pearson et al. (2019) was used to construct a modeled range of ε_{Ar} values over CO₂ concentrations of 10–50 µmol kg⁻¹ and growth rates for cultivated marine Thaumarchaeota (doubling times 21

to > 120 h; (Könneke et al., 2005; Santoro and Casciotti, 2011; Qin et al., 2014) according to:

$$\delta_{H_e} - \delta_{GDGT} = \varepsilon_{fix} - \beta \left(\frac{1}{C_e} + \frac{1}{K_{M1}} \right)$$
, where (2)

$$\beta = \frac{\mu \rho \varepsilon_{net} K_{M1}}{k_{cat1} E_1}, \text{ and } \varepsilon_{net} = \varepsilon_{fix} - \varepsilon_{HYD} - 1000(1 - \alpha).$$
 (3)

Here, δ_{He} = the *in situ* value of $\delta^{13}C_{HCO_3^-}$; $\delta_{biomass}$ = $\delta^{13}C_{GDGT}$ for crenarchaeol; ε_{fix} = the biosynthetic isotope effect for the carbon-fixing enzyme of the 3HP/4HB pathway (2.5%); ε_{HYD} = isotope effect for the slowly-catalyzed or abiotic hydration of CO₂ to HCO₃ (25%) (Zeebe, 2014); α = the temperature-dependent equilibrium fractionation factor between CO₂ and HCO₃; $\mu\rho$ = the carbon fixation rate; and K_{MI} , k_{catI} , and E_I are kinetic parameters that yield β values of approximately -45 to -48 (‰• μ M). For complete details, see Pearson et al. (in preparation). For model calculations to fit measured water column and sediment data, we calculated contours of ε_{Ar} vs. CO₂ for doubling times $(T_d = \ln(2)/\mu)$ of 48, 96, and 144 h. For reconstructing global predictions of ε_{Ar} from GLODAP data, we used only $T_d = 96$ hr, consistent with environmentally relevant strains of Thaumarchaeota (Santoro and Casciotti, 2011).

3. RESULTS

The DeepDOM cruise track (Fig. 1) traversed the equatorial and subtropical gyre surface regimes and deep water masses of North Atlantic Deep Water (NADW) and Antarctic Intermediate Water (AAIW). We analyzed samples from four stations: Station 23 at the edge of the Amazon River plume, Station 15 in the productive equatorial region, Station 7 in the South Atlantic gyre and Station 2 in the southern subtropical transition zone. Values of δ^{13} C for bulk particulate organic carbon (POC) in the 0.7–53 µm size class show a distinct minimum near the base

of the euphotic zone before returning to intermediate values at mesopelagic depths (Fig. 2 A). Values of $\delta^{13}C_{DIC}$ decrease downward from the surface to ~ 200 m and then are relatively invariant deeper in the water column (Fig. 2 B). All bulk sample data are reported in Tables S2 and S3.

In previous work we reported concentration profiles of individual core and intact polar lipid (IPL) GDGTs for large (>0.7 μ m) and small (0.3–0.7 μ m) size class filter samples (Hurley et al., 2018). Here we extracted the bulk GDGT pool (IPL and core GDGTs) for each sample, followed by acid hydrolysis and separation of individual core GDGTs for $\delta^{13}C$ analysis. The filter size classes were kept separate, but due to larger total yields from the > 0.7 μ m size class, most $\delta^{13}C_{GDGT}$ data are from this class with only a small number of values from the 0.3–0.7 μ m filters (Table S3). Regardless, there were no significant or systematic differences between data from different size classes. GDGT concentrations above depths of 80–100 m were below detection limits; therefore, isotopic GDGT data from depths between 80 m and 1000 m are reported here.

Profiles of δ^{13} C values for crenarchaeol do not covary systematically with the isotopic composition of either POC or DIC (Fig. 2). Crenarchaeol δ^{13} C values increase from the base of the photic zone through the 500 m depth horizon, and then variably increase or decrease with further depth depending on the station (Fig. 2 C). The δ^{13} C values for crenarchaeol range from -21.1 ± 0.1 to $-17.9 \pm 0.1\%$, but individual stations are significantly different from each other. For example, δ^{13} C values of crenarchaeol at the oligotrophic Station 7 (-19.2 to -20.5%) are mostly distinct from δ^{13} C values of crenarchaeol at the productive Station 15 (-17.9 to -19.5%). In many cases, δ^{13} C values for GDGT-0 and the combined minor GDGT fraction (GDGT-1, GDGT-2, and GDGT-3) agree within measurement error of crenarchaeol (Fig. S3, Table S3). The average difference between crenarchaeol and GDGT-0 or minor GDGTs across the entire dataset is 0.3%. Of the depths where δ^{13} C values for GDGT-0 and minor GDGTs differ from crenarchaeol, the offset is not systematic and may be small enough to be physiologically insignificant. Henceforth, we use δ^{13} C values from crenarchaeol in the 0.7– 53 μm size class in our data analysis as this is the largest dataset and crenarchaeol is currently thought to be restricted to the Thaumarchaeota.

The offset between $\delta^{13}C_{GDGT}$ and the $\delta^{13}C$ values of the HCO $_3^-$ component of DIC, ε_{Ar} (Eq. (1)), decreases through the water column across all sampling stations (Fig. 2 D). Values of ε_{Ar} are smallest for the productive Station 15 and largest for the oligotrophic Station 7. All four stations have generally uniform depth-dependent trends of decreasing ε_{Ar} values, and mean values at each station are distinct from each other. Consistent with qualitative predictions of the thaumarchaeal isotope flux-balance model (Eqs. (2) and (3); Pearson et al., 2019), ε_{Ar} values decrease with depth in the water column as pH decreases and CO_2 increases.

The strongest correlations between crenarchaeol ε_{Ar} values and hydrographic or isotopic water column data are for variables associated with extent of organic matter remineralization (Fig. 3). Values of ε_{Ar} correlate well (R² value \geq 0.7) with total organic carbon (TOC) concentrations (primarily a

measure of dissolved organic carbon; e.g., Carlson and Hansell, 2015), nitrate concentrations, and apparent oxygen utilization (AOU) (Fig. 3 A-C). Values of ε_{Ar} additionally correlate well with CO₂ concentrations and pH profiles averaged from the nearest GLODAP stations with similar conservative properties (i.e., salinity and temperature) (Fig. 3 D-E). These variables are all expected to relate directly to CO₂ availability as they are associated with organic matter remineralization; for example, TOC is characteristically consumed exponentially with increasing depth in the water column, thereby generating CO2 and increasing AOU, the relative oxygen deficit (Fig. S4). In contrast, ε_{Ar} values do not covary with δ^{13} C values of particulate organic carbon (POC) (Fig. 3 I) and only weakly covary ($R^2 < 0.4$) with $\delta^{13}C_{DIC}$ values, NO₂ concentrations, and absolute O₂ concentrations (Fig. 3 F-H). These relationships appear to be independent of thaumarchaeal biomass density and lipid production as they are consistent across varying in situ GDGT concentrations (Fig. 3, symbol size), and data from all four stations follow the same patterns.

4. DISCUSSION

4.1. Metabolic and ecological inferences

This study presents the first comprehensive water column profiles of $\delta^{13}C_{GDGT}$ values, providing unique insights into the metabolic function and physiology of Thaumarchaeota. The offsets between the $\delta^{13}C_{GDGT}$ values and the potential carbon sources for Thaumarchaeota are consistent with predominantly autotrophic carbon fixation, the isotope effect of which is dependent on CO₂ concentration. When interpreted in the context of CO₂- and growth ratedependent ε_{Ar} , the data also suggest that despite current uncertainties, the degree of direct organic carbon assimilation by Thaumarchaeota is small or negligible. Moreover, the similar isotopic composition of individual GDGTs within each sample - crenarchaeol, GDGT-0, and minor GDGTs (Table S3) - potentially points to a single and metabolically uniform source, rather than a mixed community that contributes differently to the pools of, e.g., GDGT-0 and crenarchaeol. Further work is required to determine if these patterns are ubiquitous throughout the open ocean, as well as to examine if they differ in coastal zones or marginal seas. Similarly, additional complementary work is required to investigate more deeply when or if metabolic or taxonomic heterogeneity may affect the potential for a paleobarometer based on ε_{Ar} values.

4.1.1. Carbon fixation in marine Thaumarchaeota

The general 13 C-enrichment in archaeal lipids relative to algal lipids (Hoefs et al., 1997; Kuypers, 2001; Schouten et al., 2013), and the discovery of the HCO $_3$ -specific hydroxypropionate/hydroxybutyrate (3HP/4HB) carbon fixation pathway in Thaumarchaeota (Berg et al., 2007; Könneke et al., 2014), led to a prediction that δ^{13} C_{GDGT} values should vary in parallel with δ^{13} C_{DIC} values, offset by a biosynthetic isotope fractionation (Pearson et al., 2016). Several factors suggested that this autotrophic pathway might have invariant fractionation. Similar δ^{13} C values

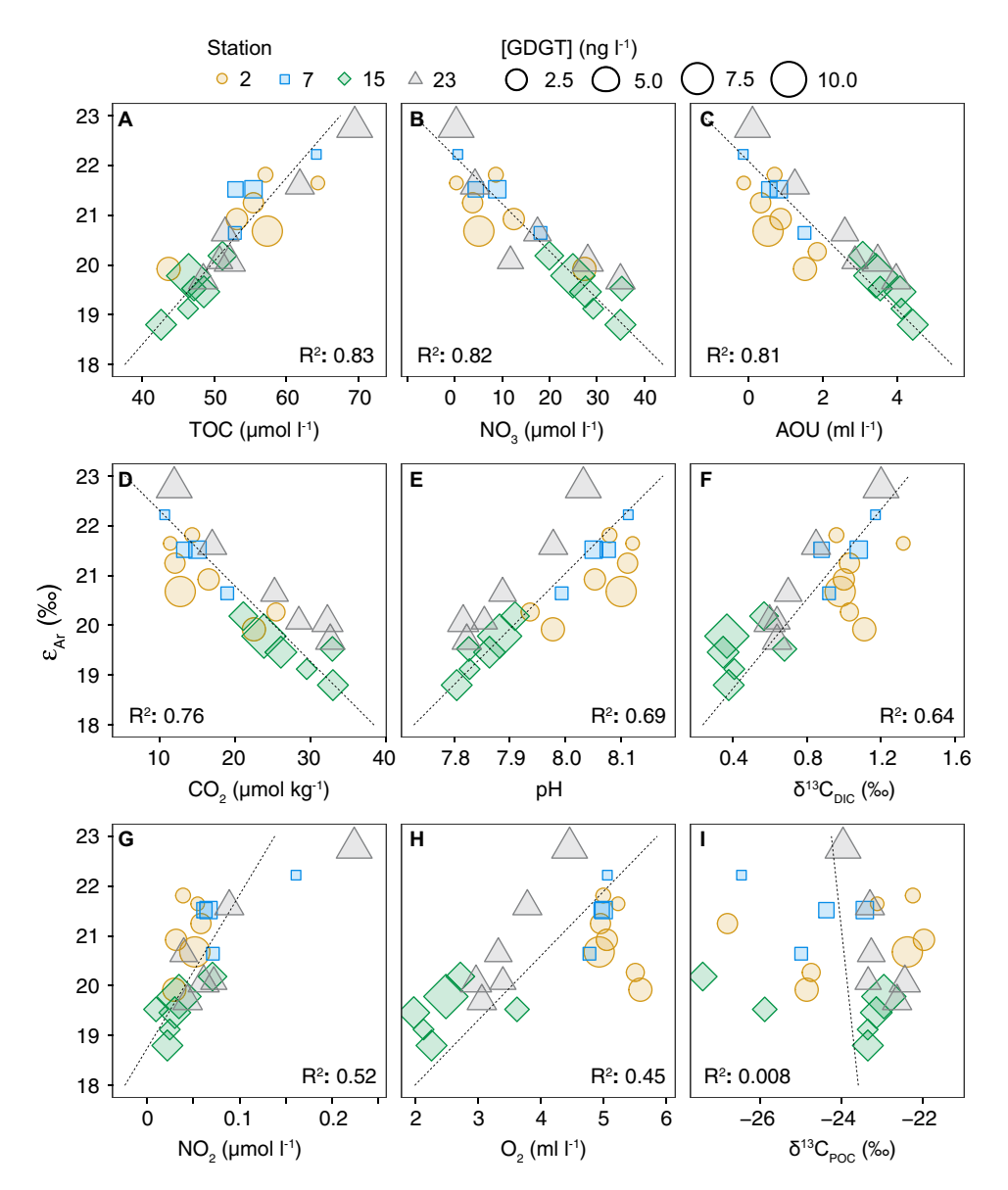


Fig. 3. Relationship between ε_{Ar} values for crenarchaeol and hydrographic or isotopic water column properties. The strongest correlations occur between ε_{Ar} and variables associated with extent of organic remineralization (A-F). Weaker correlations are observed to NO₂ and O₂ concentrations, and $\delta^{13}C_{POC}$ (G-I). Symbol sizes correspond to total GDGT concentration (ng l⁻¹) at the corresponding depth. CO₂ and pH profiles were averaged from nearest GLODAP stations (see supplement).

for bulk biomass and GDGTs rule out isotopic effects associated with variation in metabolic branching points in the 3HP/4HB cycle (Könneke et al., 2012). The specificity for HCO₃ led to the prediction that Thaumarchaeota would not be subject to the μ/[CO_{2(aq)}]-dependent effects observed in phytoplankton (Laws et al., 1995) because HCO₃ is the quantitatively dominant DIC fraction at pH ranges in the modern ocean. Additionally, some representatives of the marine group I.1a division, which includes *N. maritimus*, have an electrochemical potential-driven Na⁺/HCO₃⁻ transporter (Offre et al., 2014; Santoro et al., 2015); however, transcriptomic and proteomic data indicate the gene product for this transporter is minimally detected in *N. maritimus* (Qin et al., 2018). Consistent with these

physiological expectations, the fractionation observed in a strictly autotrophic culture of N. maritimus (calculated via mass balance from measured δ^{13} C values of biphytane sidechains of GDGTs) was ~18.7‰ (Pearson et al., 2016) and fractionation did not vary with increasing HCO $_3$ concentration in cultures grown at pH 7.5–7.6 (Könneke et al., 2012). Retrospectively, the lack of variation of the isotope effect can be understood as originating from the consistently high CO $_2$ (>40 µmol kg $^{-1}$) and HCO $_3$ (2, 4, and 8 mM) concentrations used in these culture experiments.

Previous interpretations of environmental $\delta^{13}C_{GDGT}$ values assumed a constant isotope effect for autotrophic carbon fixation in marine Thaumarchaeota and therefore invoked heterotrophy as the cause of variations in observed

 ε_{Ar} . Our current results are better explained without invoking archaeal heterotrophy; at each station sampled here, values of ε_{Ar} decrease with depth predictably in response to the increase in CO2. Previously, we suggested that changes in observed ε_{Ar} values – specifically differences between those observed in pure culture versus marine sediments - could be due to thaumarchaeal utilization of isotopically light organic compounds (Pearson et al., 2016). However, when applied to our current findings, this interpretation would require that organic carbon incorporation occurs predominantly near the base of the euphotic zone where the electron donor supply (NH₄) is highest. This interpretation is hard to reconcile as it would seem energetically advantageous to preferentially use organic carbon compounds in deeper waters when the NH₄⁺ supply is low. Similarly, a greater need for substrate and energy could be used to argue that organic carbon assimilation should be greatest at the oligotrophic Station 7 (the station with ε_{Ar} values most similar to $\delta^{13}C_{POC}$ values), but it still would not explain why values of ε_{Ar} get smaller (more "autotrophic") in the deeper, more NH₄⁺-poor waters. In sum, the patterns of ε_{Ar} with depth and between stations cannot be easily reconciled with a scenario of varying degrees of archaeal community heterotrophy.

Early inquiries into the metabolic capabilities of Thaumarchaeota revealed that natural archaeal populations were able to take up labeled amino acids (Ouverney and Fuhrman, 2000; Teira et al., 2004; Herndl et al., 2005). However, this approach did not distinguish between uptake of amino acids as a carbon source versus other cellular uses. Recognition of the capacity of Thaumarchaeota to oxidize urea (Tolar et al., 2017; Qin et al., 2017; Santoro et al., 2019; Kitzinger et al., 2018) suggested the potential for a broader range of organic nitrogen energy sources. The specialized machinery used to cleave urea for ammonia oxidation could be applied to cleave other compounds; or alternatively a promiscuous ammonia monooxygenase could accept a diversity of substrates, meaning that general uptake of amino acids could potentially be assigned to energy metabolism, rather than carbon assimilation. Recently it also was determined that coastal strains that were originally thought to be obligate mixotrophs (Qin et al., 2014) are instead carrying out a hydrogen peroxide detoxification mechanism in which organic carbon is a necessary co-metabolite but is not incorporated into lipids (Kim et al., 2016). Significant uptake of ¹³C-labeled acetate compared to 13C-labeled inorganic carbon has been observed in stable isotope probing (SIP) experiments targeting the TACK, the super phylum that includes Thaumarchaeota (Seyler et al., 2018), although it is unclear if the relatively short (48 h) incubation times and lack of added NH₄ to serve as electron donor may have impacted the populations. Additional work using cell-specific approaches such as nano-scale secondary ion mass spectrometry (nano-SIMS) may be necessary for a better understanding of the heterotrophic potential of marine Thaumarchaeota.

4.1.2. Taxonomic sources of GDGTs

Potential variations in the taxonomic sources of GDGTs have important implications for the paleoceanographic util-

ity of these lipids. Group I.1a Thaumarchaeota are believed to be the major source of GDGTs in marine systems, and in particular, biosynthesis of crenarchaeol is currently thought to be restricted to the Thaumarchaeota and possibly associated specifically with ammonia oxidation (de la Torre et al., 2008; Schouten et al., 2008; Pitcher et al., 2010). Recently Lincoln et al. (2014) proposed that Marine Group II Euryarchaeota are also a significant source of GDGTs in the water column, garnering some debate (Schouten et al., 2014). Our data suggest that GDGTs are primarily derived from a uniform metabolic source due to the similar δ^{13} C values for GDGT-0 and crenarchaeol. Either the water column inventory of GDGTs at these locations is derived almost exclusively from Thaumarchaeota, or the carbon metabolism of marine communities of Thaumarchaeota and Euryarchaeota is indistinguishable, since both groups should contribute significantly to the inventory of GDGT-0.

In addition to our $\delta^{13}C_{GDGT}$ data, other arguments may suggest that major contributions from Euryarchaeota are unlikely. Molecular surveys show different vertical distributions of Euryarchaeota and Thaumarchaeota, with Euryarchaeota making up a larger proportion of archaea in surface waters (Massana et al., 1997; Massana et al., 1998; Massana et al., 2000) and Thaumarchaeota dominating at the base of the photic zone and below (Francis et al., 2005; Beman et al., 2008; Church et al., 2010; Santoro et al., 2010). A primarily heterotrophic physiology of MG II Eurvarchaeota has been inferred from metagenomics (Iverson et al., 2012; Zhang et al., 2015). Therefore, a significant source of GDGTs from Euryarchaeota with a different carbon source should result in the divergence of GDGT-0 and crenarchaeol δ¹³C values (e.g., Pancost et al., 2000), something which is not seen in our data. Similarly, a quantitatively significant inventory of MG II Euryarchaeota in surface waters is not consistent with our previously reported GDGT concentration data, which indicates that both IPL and core GDGT concentrations in the upper 50 m of the water column generally make up less than 2% of the total GDGT inventory while concentrations from 80 m and below make up > 98% of the total GDGT inventory (Hurley et al., 2018).

4.2. Thaumarchaeal isotope flux-balance model

Our newly-developed thaumarchaeal isotope model (Eqs. (2) and (3); Pearson et al., 2019) predicts that the value of ε_{Ar} is CO₂-dependent due to the interplay between diffusive entry of extracellular CO₂ and slow intracellular conversion of that CO₂ to the necessary biosynthetic substrate, HCO₃. This model suggests the relationship between ε_{Ar} and CO₂ is better represented as curvilinear (Fig. 4 A) rather than linear (Fig. 3 D). Water column ε_{Ar} values from the four South Atlantic stations are consistent with the predicted directionally of the model, *i.e.*, smaller ε_{Ar} values at high CO₂ concentrations, while nearly all values fit within contours that suggest *in situ* community doubling times between 2–6 days (Fig. 4 A, grey contours). We suggest adopting a mean doubling time of 96 h (4 days) as a reasonable approximation based on these data. A doubling time

of 4 days is also generally consistent with observed growth rates in environmentally-relevant cultures of Thaumarchaeota (Santoro and Casciotti, 2011). Importantly, the relationship between water column $\varepsilon_{\rm Ar}$ values and CO₂ concentrations is continuous across all sampling stations – all samples fit within the same curves – suggesting that CO₂ concentration is a controlling variable. However, this dataset describes the relationship over a relatively limited working range, with values of $\varepsilon_{\rm Ar}$ decreasing by ~4‰ over a 25 µmol kg⁻¹ increase in dissolved CO₂.

We incorporated water column ε_{Ar} values into a previously published export model (Hurley et al., 2018) to estimate the ε_{Ar} signal exported to marine sediments (Table S5). This model, based on comparing massweighted export calculations to the GDGT distributions (GDGT-2/3 ratio) observed in nearest sediments (Tierney and Tingley, 2015), suggests that GDGTs are primarily exported from between 80-250 m. We then used the results of the thaumarchaeal isotope model to convert exported ε_{Ar} values into an exported CO₂ signal (Fig. 4 A, colored bars). Finally, we calculated pCO₂ levels (Fig. 4 B) based on the exported CO₂ signal, and in situ temperature, pressure, and pH at the depth of export. These estimates show that exported ε_{Ar} values should reflect the depth of maximum GDGT production, i.e., the largest symbol size for each station (Fig. 4 A) and thus dissolved CO₂ in this depth range. The CO₂ concentration values predicted from exported GDGTs are all < 15 μ mol kg⁻¹ for Stations 2, 7, and 23; while the value from Station 15 is > 20 μ mol kg⁻¹. The reconstructed CO₂ concentrations from Stations 2, 7, and 23 therefore correspond to calculated pCO₂ levels of 300–

400 ppm, consistent with $p\text{CO}_2$ levels of the past century, while the productive equatorial Station 15 predicts a higher $p\text{CO}_2$ level of \sim 600 ppm (Fig. 4 B). We recognize that CO_2 concentrations at our proposed depths of export are higher than surface concentrations due to remineralization of organic matter, but we use this approximation as a starting point for exploring the predictive capabilities of the ε_{Ar} -CO₂ relationship.

Our observed water column profiles suggest that if growth rate and other aspects of community physiology are relatively constant properties of the marine Thaumarchaeota community, ε_{Ar} should be predictable from in situ dissolved CO₂ concentrations using a single parameterization of the isotope model (Eqs. (2) and (3)). To examine this idea, we used the model to predict the range of global ε_{Ar} values corresponding to the average dissolved CO₂ concentrations between 80-250 m depth, the predicted export window corresponding to the primary thaumarchaeal habitat (Fig. 5). The calculation used a uniform doubling time of 96 h (4 days) and all other parameters were as specified previously (e.g., Fig. 4). The model predicts that ε_{Ar} values should be smaller (19-20%) in upwelling regions and larger (>22‰) in gyre regions. Estimates of the net exported signal (Fig. 5B, filled diamonds; Fig. S6; Table S5) show how the GDGTs accumulating in sediments could preserve a signal of dissolved CO₂ concentrations from the subsurface with an overall signal range of ~3% in the modern ocean. Although small, a 3% signal is 20 times larger than our average measurement precision (1σ) for water column δ¹³C_{GDGT} values and 12–15 times larger than our measurement precision for sediment samples, which are more diffi-

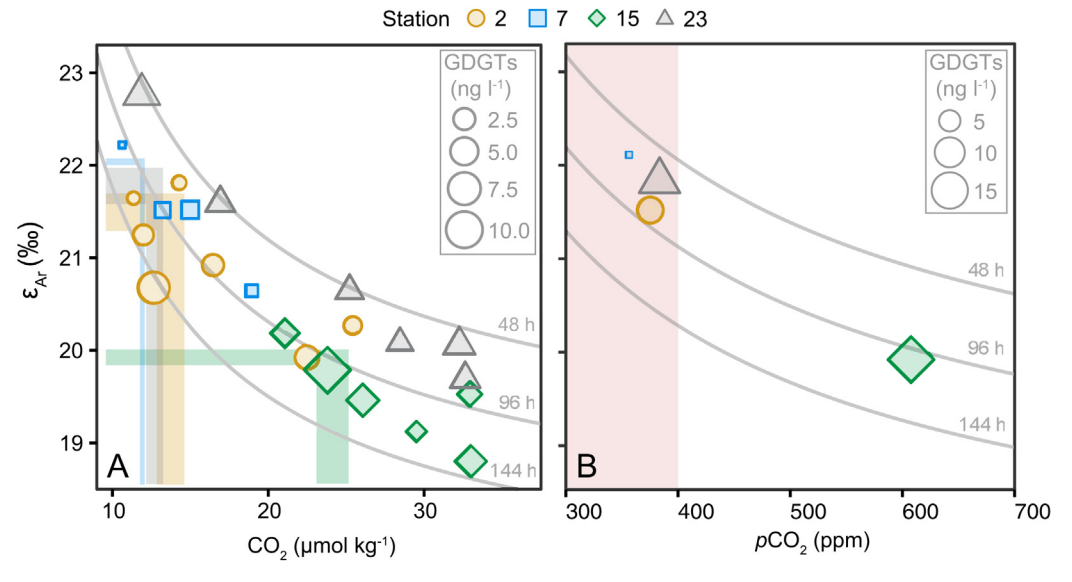


Fig. 4. Sensitivity of ε_{Ar} to CO₂ concentration. (A) The thaumarchaeal carbon isotope model (Eqs. (2) and (3)) is consistent with the observed relationship between ε_{Ar} values for crenarchaeol and CO₂ concentration in the water column. Symbols sizes represent total GDGT concentrations (ng l⁻¹) at the corresponding depth. Grey contours represent model results corresponding to cell doubling times of 48 h, 96 h, and 144 h (2, 4, and 6 days). Filled bars represent estimates of the net signal exported to sediments, based on the lipid export model in Hurley et al. (2018) and an assumed doubling time of 96 h; also see Fig. S6. (B) Exported CO₂ signal replotted as the resulting estimates of atmospheric pCO₂. Grey contours represent conversion of the CO₂ model to pCO₂ based on 15 °C seawater, pH 8.0, a temperature-sensitive Henry's Law constant (Zeebe and Wolf-Gladrow, 2001), and assuming equilibrium with the atmosphere. Red shaded area (300–400 ppm) approximates pCO₂ levels of the past century.

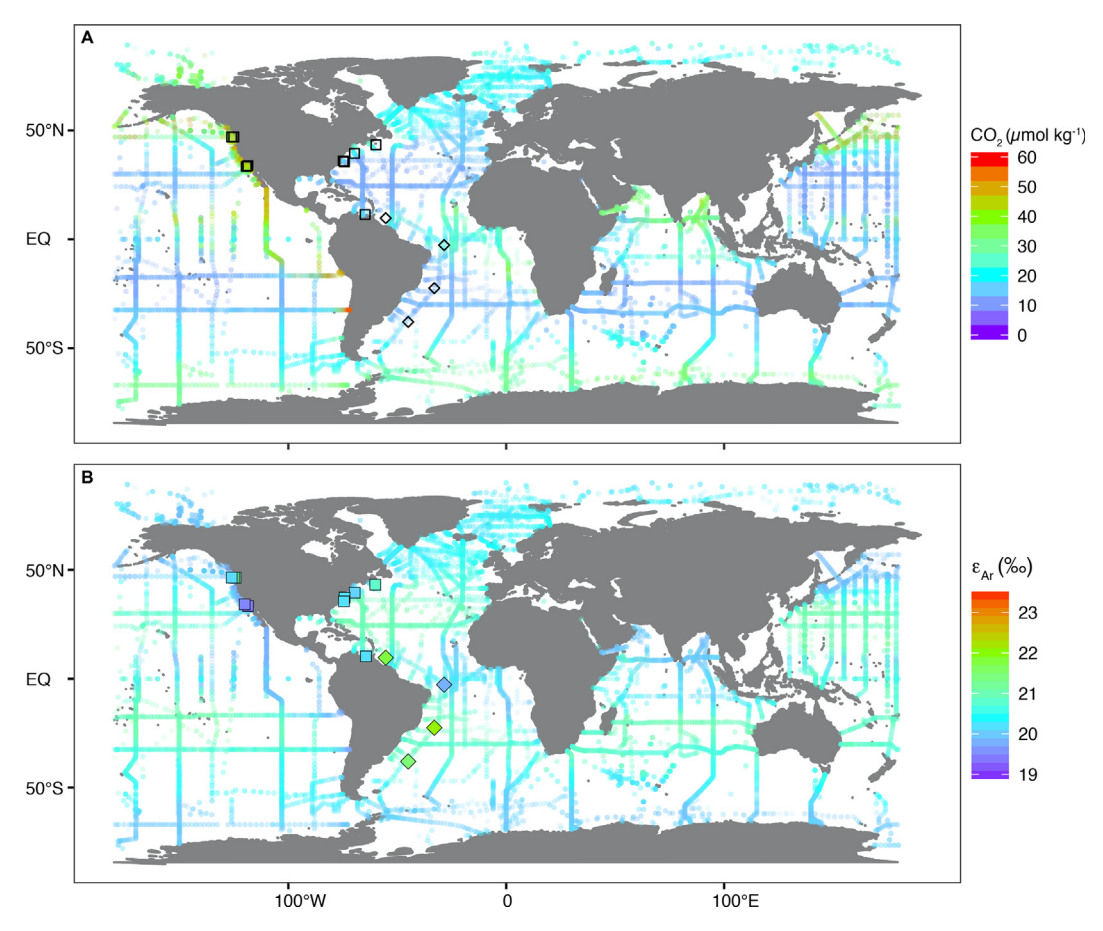


Fig. 5. Global distribution of predicted ε_{Ar} values. (A) Average CO₂ concentrations from water depths of 80–250 m in the GLODAP database (small color points). Large open symbols show the locations of the four cruise stations (diamonds) and the sediment core-top locations sampled in Pearson et al. (2016) (squares). (B) Values of ε_{Ar} predicted from the thaumarchaeal carbon isotope model based on CO₂ concentrations shown above and assuming $T_d = 96$ h (small points). Large filled symbols show the ε_{Ar} values observed for the four cruise stations (diamonds) and for the sediment core-top locations sampled in Pearson et al. (2016) (squares).

cult to obtain in high purity relative to background carbon contamination (Pearson et al., 2016; Polik et al., 2018).

The $\delta^{13}C_{GDGT}$ values from marine sediments reported in Pearson et al. (2016) provide an independent check on these predictions. To calculate ε_{Ar} values using δ^{13} C values of crenarchaeol from previously reported core top sediments, we located the nearest station with $\delta^{13}C_{\rm DIC}$ values from the GLODAP dataset (Table S4). We then calculated DIC speciation and $\delta^{13}C_{HCO_3^-}$ values to calculate ε_{Ar} according to Eq. (1). In concert, we also determined the nearest station with CO₂ concentrations from GLODAP, stations which were typically much closer to the actual sediment sampling locations; the farthest had a maximum distance of 150 km from the sediment location (Table S4). We used the average CO₂ concentration between 80-250 m for these nearest stations to model ε_{Ar} values, again with a corresponding doubling time of 4 days (Fig. 5 B, filled squares). Modeled and calculated ε_{Ar} values agree within a 1% error range at all sediment locations (Fig. 6) except for two samples from a coastal Washington (WA) margin transect, the shallowest of which had a water column depth of only 75 m. A more systematic sampling approach including water column $\delta^{13}C_{DIC}$, DIC speciation, pH, and temperature – as well as a much larger suite of core top sediment locations – is needed to test whether or under what conditions the ε_{Ar} signal preserved in sediments is consistent with predicted values of ε_{Ar} from the 80–250 m horizon of the open marine water column.

4.3. Prospects for paleobarometry

The range in ε_{Ar} values we observed in the modern marine water column exceeds the present range of $\delta^{13}C_{DIC}$ values. Therefore, currently ε_{Ar} cannot be used directly to reconstruct values of $\delta^{13}C_{DIC}$ without also accounting for the CO_2 and μ dependence of ε_{Ar} (Eqs. (2) and (3)). However, under conditions of atmospheric $pCO_2 > 1500$ ppm, for example during the Eocene hyperthermals, the ε_{Ar} proxy would approach saturation (*i.e.*, approach its minimum value) and changes in $\delta^{13}C$ values of GDGTs would more closely reflect the change in total ocean ^{13}C inventory, making direct reconstruction of $\delta^{13}C_{DIC}$ feasible.

For paleobarometry applications, the results from the modern marine water column provide initial support for the use of the thaumarchaeal ε_{Ar} proxy to reconstruct past

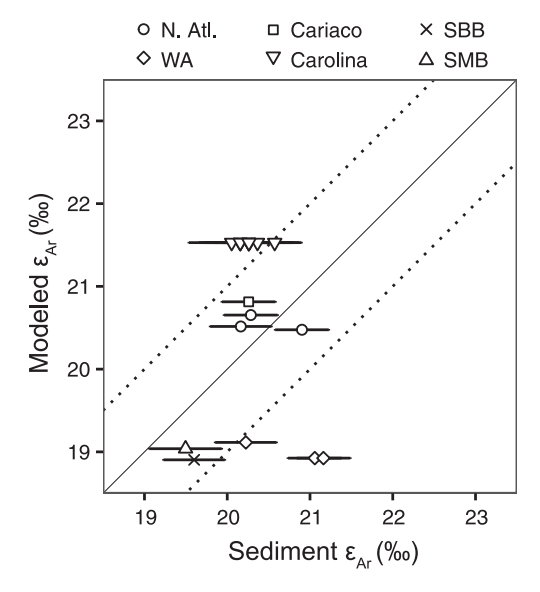


Fig. 6. Values of ε_{Ar} predicted from the thaumarchaeal carbon isotope model (Eqs. (2) and (3)) are partially consistent with the observed ε_{Ar} values from the sediment core-top locations sampled in Pearson et al. (2016). Modeled ε_{Ar} values are estimated from the average CO₂ concentration between 80–250 m at the nearest GLODAP station (Table S4) and assuming $T_d=96$ h. Sediment ε_{Ar} values are calculated according Eq. (1), using the average $\delta^{13}C_{HCO_3}$ value between 80–250 m at the nearest GLODAP station with $\delta^{13}C_{DIC}$ data. Dashed lines represent a $\pm 1\%$ region around the 1:1 (solid) line. Uncertainties for the sediment ε_{Ar} values assume a $\delta^{13}C_{HCO_3}$ uncertainty of 0.3%.

 pCO_2 levels when atmospheric CO_2 content was ≤ 4 times the pre-anthropogenic Holocene level (Pearson et al., 2019), provided CO₂ concentrations at the depth of GDGT production and export can be related to atmospheric CO₂ levels (Fig. S5). The predictions of the ε_{Ar} model, particularly the sensitivity to CO₂ availability, is evident across all water columns sampled here. Values of ϵ_{Ar} are smaller at higher dissolved CO2 concentrations, forming one continuous relationship spanning $\sim 25~\mu mol~kg^{-1}$ of dissolved CO₂. However the corresponding \sim 4% sensitivity in ε_{Ar} represents a small working range, particularly considering an error estimate of $\sim 1\%$ for preliminary ε_{Ar} values reconstructed from modern sediments (Fig. 6). While the current water column and sediment core top data define the predicted global distribution of ε_{Ar} values as having the same 4% range as the specific particulate organic matter data obtained from the Southwest Atlantic water column, further work is needed to refine the full range of possible ε_{Ar} values.

Current understanding of archaeal lipid export indicates that the $\varepsilon_{\rm Ar}$ signal reaching sediments primarily would reflect the dissolved CO₂ concentration at the depth of maximum GDGT concentrations (Fig. 4). This depth typically is centered around ~100 m and spans generally 80–250 m (Hurley et al., 2018). In other organic paleobarometers based on photoautotrophic organisms, namely the alkenone and phytane paleobarometers (Laws et al., 1995; Pagani et al., 2005; Witkowski et al., 2018), conversion between photic zone dissolved CO₂ concentrations and

pCO₂ levels is relatively straightforward. Dissolved CO₂ in the surface ocean is assumed to be in equilibrium with atmospheric CO2 and a Henry's law constant can be used to convert between the two CO2 reservoirs. Relating dissolved CO2 at the depth habitat of Thaumarchaeota to pCO₂ is more difficult. Dissolved CO₂ concentrations in this depth range reflect both atmospheric pCO₂ levels and CO₂ released during the respiration of organic matter. In the GLODAP dataset, the distribution of pCO₂ levels calculated from the concentration of dissolved CO₂ between 80–250 m is skewed towards higher than modern pCO₂ levels, although the median value is the "correct" value of ~ 390 ppm (Fig. S5). The pCO₂ values predicted from exported GDGTs reflect this global distribution (Fig. 4 B). The median value of pCO_2 levels calculated from dissolved CO₂ in surface waters is ~ 350 ppm (Fig. S5). Estimates from both the surface and subsurface would therefore approximate pCO_2 levels over the past century (300-400 ppm). When selecting stations for GDGT paleobarometry, the most critical factor likely will be to avoid productive upwelling and other known disequilibrium locations, although this is an important and known challenge that affects all organic, CO₂-dependent paleobarometers.

5. CONCLUSIONS

An isotope flux-balance model based on kinetic modeling of 3HP/4HB pathway physiology (Part I companion paper; Pearson et al., 2019) suggests that carbon isotope fractionation (ε_{Ar}) in marine Thaumarchaeota should be sensitive to growth rate (μ) and CO₂ availability under conditions of atmospheric pCO2 < 4 times the preanthropogenic Holocene level. Here we showed that values of $\delta^{13}C_{GDGT}$ from four water column profiles in the Southwest and Equatorial Atlantic Ocean support the premise of that model in both qualitative trends and absolute magnitude. Values of $\delta^{13}C_{GDGT}$ increase with depth in the water column, in contrast to the simultaneous decrease in $\delta^{13}C_{DIC}$ values. The result is a decrease in the observed total biosynthetic isotope effect (ε_{Ar}) as CO_2 concentrations increase with depth. The ε_{Ar} signal reaching marine sediments therefore has the potential to record dissolved CO2 concentrations corresponding to the depth of maximum thaumarchaeal export, i.e., around the base of the photic zone. CO₂ concentrations in this portion of the water column reflect both atmospheric pCO₂ levels and CO₂ released during the respiration of organic matter, but in relatively open ocean (and non-upwelling) sites, the dominant influence is the atmosphere. This implies that values of ε_{Ar} could serve as a pCO_2 paleobarometer.

The greatest uncertainties for calculating ε_{Ar} and therefore pCO_2 may stem not from the measurement of the $\delta^{13}C$ value of the archaeal biomass via the lipid crenarchaeol, but rather from the challenge of characterizing the isotopic history of coeval DIC and therefore bicarbonate. This value would need to be reconstructed from sedimentary foraminiferal calcite or total carbonate data, with concomitant assumptions about calcite $\Leftrightarrow CO_3^{2-} \Leftrightarrow HCO_3^{-}$ isotopic distribution, the associated in situ temperatures, and the specific isotopic properties at the base of the photic

zone where most thaumarchaeal export production originates. If these challenges can be overcome, ε_{Ar} may prove useful for pCO_2 paleobarometry.

ACKNOWLEDGMENTS

We thank Boswell Wing, Sebastian Kopf, David Johnston, and Eric Ellison for valuable discussions. We thank Joe Werne for editorial assistance and three anonymous reviewers for valuable comments. We are grateful to the crew, chief scientists E. Kujawinski and K. Longnecker, and the scientific shipboard part of *R/V* Knorr cruise KN201-04. Funding for the cruise was provided by the National Science Foundation (NSF-1154320 to E. Kujawinski and K. Longnecker, WHOI). AP, SJH, and FE acknowledge funding from the National Science Foundation (NSF-1129343, NSF-1702262), the Gordon and Betty Moore Foundation, the NASA Astrobiology Institute and from the Agouron Institute (to S.J. H.). KG and APM were supported through the NOSAMS Cooperative Agreement (NSF-1239667).

APPENDIX A. SUPPLEMENTARY MATERIAL

Supplementary data to this article can be found online at https://doi.org/10.1016/j.gca.2019.06.043.

REFERENCES

- Beman J. M., Popp B. N. and Francis C. A. (2008) Molecular and biogeochemical evidence for ammonia oxidation by marine Crenarchaeota in the Gulf of California. *ISME J.* **2**, 429–441.
- Berg I. A., Kockelkorn D., Buckel W. and Fuchs G. (2007) A 3hydroxypropionate/4-hydroxybutyrate autotrophic carbon dioxide assimilation pathway in Archaea. Science 318, 1782– 1786
- Carlson C. A. and Hansell D. A. (2015) Chapter 3 DOM Sources, Sinks, Reactivity, and Budgets. Academic Press, Boston, pp. 65– 126
- Church M. J., Wai B., Karl D. M. and DeLong E. F. (2010) Abundances of crenarchaeal *amoA* genes and transcripts in the Pacific Ocean. *Environ. Microbiol.* **12**, 679–688.
- DeLong E. F. (1992) Archaea in coastal marine environments. *PNAS* **89**, 5685–5689.
- Elling F. J., Könneke M., Nicol G. W., Stieglmeier M., Bayer B., Spieck E., de la Torre J. R., Becker K. W., Thomm M., Prosser J. I., Herndl G. J., Schleper C. and Hinrichs K.-U. (2017) Chemotaxonomic characterisation of the thaumarchaeal lipidome. *Environ. Microbiol.* 19, 2681–2700.
- Francis C. A., Roberts K. J., Beman J. M., Santoro A. E. and Oakley B. B. (2005) Ubiquity and diversity of ammonia-oxidizing archaea in water columns and sediments of the ocean. *PNAS* **102**, 14683–14688.
- Freeman K. H. and Pagani M. (2005) Alkenone-Based Estimates of Past CO2 Levels: A Consideration of Their Utility Based on an Analysis of Uncertainties Available at:. Springer New York, New York, NY, pp. 35–61.
- Frigaard N.-U., Martinez A., Mincer T. J. and DeLong E. F. (2006) Proteorhodopsin lateral gene transfer between marine planktonic Bacteria and Archaea. *Nature* 439, 847–850.
- Fuhrman J., McCallum K. and Davis A. (1992) Novel major archaebacterial group from marine plankton. *Nature* 356, 148– 149.
- Gospodinova K., McNichol A. P., Gagnon A. and Shah Walter S. R. (2015) Rapid extraction of dissolved inorganic carbon from

- seawater and groundwater samples for radiocarbon dating. Limnol. Oceanogr: Methods 14, 24–30.
- Herndl G. J., Reinthaler T., Teira E., van Aken H., Veth C., Pernthaler A. and Pernthaler J. (2005) Contribution of Archaea to total prokaryotic production in the deep Atlantic Ocean. Appl. Environ. Microbiol. 71, 2303–2309.
- Hoefs M., Schouten S., DeLeeuw J., King L., Wakeham S. and Sinninghe Damsté J. S. (1997) Ether lipids of planktonic archaea in the marine water column. *Appl. Environ. Microbiol.* 63, 3090–3095.
- Hurley S. J., Lipp J. S., Close H. G., Hinrichs K.-U. and Pearson A. (2018) Distribution and export of isoprenoid tetraether lipids in suspended particulate matter from the water column of the Western Atlantic Ocean. Org. Geochem. 116.
- Ingalls A. E., Shah S. R., Hansman R. L., Aluwihare L. I., Santos G. M., Druffel E. R. M. and Pearson A. (2006) Quantifying archaeal community autotrophy in the mesopelagic ocean using natural radiocarbon. *PNAS* 103, 6442–6447.
- Iverson V., Morris R. M., Frazar C. D., Berthiaume C. T., Morales R. L. and Armbrust E. V. (2012) Untangling Genomes from Metagenomes: Revealing an Uncultured Class of Marine Euryarchaeota. Science 335, 587–590.
- Jenkyns H. C., Schouten-Huibers L., Schouten S. and Sinninghe Damsté J. S. (2012) Warm Middle Jurassic-Early Cretaceous high-latitude sea-surface temperatures from the Southern Ocean. Climate Past 8, 215–226.
- Karner M. B., DeLong E. F. and Karl D. M. (2001) Archaeal dominance in the mesopelagic zone of the Pacific Ocean. *Nature* 409, 507–510.
- Kim J.-G., Park S.-J., Sinninghe Damsté J. S., Schouten S., Rijpstra W. I. C., Jung M.-Y., Kim S.-J., Gwak J.-H., Hong H., Si O.-J., Lee S., Madsen E. L. and Rhee S.-K. (2016) Hydrogen peroxide detoxification is a key mechanism for growth of ammonia-oxidizing archaea. *PNAS* 113, 7888–7893.
- Kitzinger K., Padilla C. C., Marchant H. K., Hach P. F., Herbold C. W., Kidane A. T., Könneke M., Littmann S., Mooshammer M., Niggemann J., Petrov S., Richter A., Stewart F. J., Wagner M., Kuypers M. M. M. and Bristow L. A. (2018) Cyanate and urea are substrates for nitrification by Thaumarchaeota in the marine environment Available at:. *Nat. Microbiol.*
- Könneke M., Bernhard A. E., de la Torre J. R., Walker C. B., Waterbury J. B. and Stahl D. A. (2005) Isolation of an autotrophic ammonia-oxidizing marine archaeon. *Nature* **437**, 543–546.
- Könneke M., Lipp J. S. and Hinrichs K.-U. (2012) Carbon isotope fractionation by the marine ammonia-oxidizing archaeon Nitrosopumilus maritimus. *Org. Geochem.* **48**, 21–24.
- Könneke M., Schubert D. M., Brown P. C., Hügler M., Standfest S., Schwander T., Schada von Borzyskowski L., Erb T. J., Stahl D. A. and Berg I. A. (2014) Ammonia-oxidizing archaea use the most energy-efficient aerobic pathway for CO₂ fixation. *PNAS* 111, 8239–8244.
- Kujawinski, E., Longnecker, K., 2013. Dissolved Organic Matter Composition in the Deep Atlantic Ocean: CTD. Available at: http://www.bco-dmo.org/dataset/481164/data.
- Kuypers M. M. M. (2001) Massive expansion of marine archaea during a mid-cretaceous oceanic anoxic event. Science 293, 92– 95
- de la Torre J. R., Walker C. B., Ingalls A. E., Könneke M. and Stahl D. A. (2008) Cultivation of a thermophilic ammonia oxidizing archaeon synthesizing crenarchaeol. *Environ. Micro-biol.* 10, 810–818.
- Laws E. A., Popp B. N., Bidigare R. R., Kennicutt M. C. and Macko S. A. (1995) Dependence of phytoplankton carbon isotopic composition on growth rate and [CO_{2]aq}: Theoretical

- considerations and experimental results. *Geochim. Cosmochim. Acta* **59**, 1131–1138.
- Lincoln S. A., Wai B., Eppley J. M., Church M. J., Summons R. E. and DeLong E. F. (2014) Planktonic Euryarchaeota are a significant source of archaeal tetraether lipids in the ocean. PNAS 111, 9858–9863.
- Martin-Cuadrado A.-B., Garcia-Heredia I., Moltó A. G., López-Úbeda R., Kimes N., López-García P., Moreira D. and Rodriguez-Valera F. (2014) A new class of marine Euryarchaeota group II from the mediterranean deep chlorophyll maximum. ISME J. 9, 1619.
- Massana R., DeLong E. F. and Pedros-Alio C. (2000) A few cosmopolitan phylotypes dominate planktonic archaeal assemblages in widely different Oceanic Provinces. *Appl. Environ. Microbiol.* 66, 1777–1787.
- Massana R., Murray A., Preston C. and DeLong E. (1997) Vertical distribution and phylogenetic characterization of marine planktonic Archaea in the Santa Barbara Channel. *Appl. Environ. Microbiol.* 63, 50–56.
- Massana R., Taylor L. T., Murray A. E., Wu K. Y., Jeffrey W. H. and DeLong E. F. (1998) Vertical distribution and temporal variation of marine planktonic archaea in the Gerlache Strait, Antarctica, during early spring. *Limnol. Oceanogr.* 43, 607–617.
- Mook W. G., Bommerson J. C. and Staverman W. H. (1974) Carbon isotope fractionation between dissolved bicarbonate and gaseous carbon dioxide. *Earth Planet. Sci. Lett.* 22, 169– 176.
- Offre P., Kerou M., Spang A. and Schleper C. (2014) Variability of the transporter gene complement in ammonia-oxidizing archaea. *Trends Microbiol.* **22**, 665–675.
- Olsen A., Key R. M., van Heuven S., Lauvset S. K., Velo A., Lin X., Schirnick C., Kozyr A., Tanhua T., Hoppema M., Jutterström S., Steinfeldt R., Jeansson E., Ishii M., Pérez F. F. and Suzuki T. (2016) The Global Ocean Data Analysis Project version 2 (GLODAPv2) an internally consistent data product for the world ocean. Earth Syst. Sci. Data 8, 297–323.
- Orsi W. D., Smith J. M., Wilcox H. M., Swalwell J. E., Carini P., Worden A. Z. and Santoro A. E. (2015) Ecophysiology of uncultivated marine euryarchaea is linked to particulate organic matter. *ISME J.* **9**, 1747–1763.
- Ouverney C. C. and Fuhrman J. A. (2000) Marine planktonic archaea take up amino acids. Appl. Environ. Microbiol. 66, 4829–4833.
- Pagani M., Zachos J. C., Freeman K. H., Tipple B. and Bohaty S. (2005) Marked decline in atmospheric carbon dioxide concentrations during the paleogene. *Science* 309, 600.
- Pancost R. D., van Geel B., Baas M. and Damsté J. S. S. (2000) δ^{13} C values and radiocarbon dates of microbial biomarkers as tracers for carbon recycling in peat deposits. *Geology* **28**, 663–666.
- Pearson A., Hurley S. J., Elling F. J. and Wilkes E. B. (2019) CO₂-dependent carbon isotope fractionation in Archaea, Part I: Modeling the 3HP/4HB pathway. *Geochimica et Cosmochimica Acta* 261, 368–382. https://doi.org/10.1016/j.gca.2019.06.042.
- Pearson A., Hurley S. J., Shah Walter S. R., Kusch S., Lichtin S. and Zhang Y. G. (2016) Stable carbon isotope ratios of intact GDGTs indicate heterogeneous sources to marine sediments. *Geochim. Cosmochim. Acta* 181, 18–35.
- Pearson A. and Ingalls A. E. (2013) Assessing the Use of Archaeal Lipids as Marine Environmental Proxies. Annu. Rev. Earth Planet. Sci. 41, 359–384.
- Pitcher A., Rychlik N., Hopmans E. C., Spieck E., Rijpstra W. I. C., Ossebaar J., Schouten S., Wagner M. and Damsté J. S. S. (2010) Crenarchaeol dominates the membrane lipids of Candi-

- datus Nitrososphaera gargensis, a thermophilic group I.1b Archaeon. ISME J. 4, 542–552.
- Polik C. A., Elling F. J. and Pearson A. (2018) Impacts of paleoecology on the TEX₈₆ sea surface temperature proxy in the pliocene-pleistocene mediterranean sea. *Paleoceanogr. Paleoclimatol.* 33, 1472–1489.
- Qin W., Amin S. A., Lundeen R. A., Heal K. R., Martens-Habbena W., Turkarslan S., Urakawa H., Costa K. C., Hendrickson E. L., Wang T., Beck D. A., Tiquia-Arashiro S. M., Taub F., Holmes A. D., Vajrala N., Berube P. M., Lowe T. M., Moffett J. W., Devol A. H., Baliga N. S., Arp D. J., Sayavedra-Soto L. A., Hackett M., Armbrust E. V., Ingalls A. E. and Stahl D. A. (2018) Stress response of a marine ammonia-oxidizing archaeon informs physiological status of environmental populations. *ISME J.* 12, 508.
- Qin W., Amin S. A., Martens-Habbena W., Walker C. B., Urakawa H., Devol A. H., Ingalls A. E., Moffett J. W., Armbrust E. V. and Stahl D. A. (2014) Marine ammoniaoxidizing archaeal isolates display obligate mixotrophy and wide ecotypic variation. *PNAS* 111, 12504–12509.
- Qin W., Heal K. R., Ramdasi R., Kobelt J. N., Martens-Habbena W., Bertagnolli A. D., Amin S. A., Walker C. B., Urakawa H., Könneke M., Devol A. H., Moffett J. W., Armbrust E. V., Jensen G. J., Ingalls A. E. and Stahl D. A. (2017) Nitrosopumilus maritimus gen. nov., sp. nov., Nitrosopumilus cobalaminigenes sp. nov., Nitrosopumilus oxyclinae sp. nov., and Nitrosopumilus ureiphilus sp. nov., four marine ammonia-oxidizing archaea of the phylum Thaumarchaeota. *Int. J. Syst. Evol. Microbiol.* 67, 5067–5079.
- Santoro A. E. and Casciotti K. L. (2011) Enrichment and characterization of ammonia-oxidizing archaea from the open ocean: phylogeny, physiology and stable isotope fractionation. *ISME J.* 5, 1796–1808.
- Santoro A. E., Casciotti K. L. and Francis C. A. (2010) Activity, abundance and diversity of nitrifying archaea and bacteria in the central California Current. *Environ. Microbiol.* 12, 1989– 2006
- Santoro A. E., Dupont C. L., Richter R. A., Craig M. T., Carini P., McIlvin M. R., Yang Y., Orsi W. D., Moran D. M. and Saito M. A. (2015) Genomic and proteomic characterization of "Candidatus Nitrosopelagicus brevis": An ammonia-oxidizing archaeon from the open ocean. PNAS 112, 1173–1178.
- Santoro A. E., Richter R. A. and Dupont C. L. (2019) Planktonic Marine Archaea. Annu. Rev. Mar. Sci. 11, 131–158.
- Schouten S., Hoefs M. J. L., Koopmans M. P., Bosch H.-J. and Sinninghe Damsté J. S. (1998) Structural characterization, occurrence and fate of archaeal ether-bound acyclic and cyclic biphytanes and corresponding diols in sediments. *Org. Geochem.* 29, 1305–1319.
- Schouten S., Hopmans E. C., Baas M., Boumann H., Standfest S., Könneke M., Stahl D. A. and Sinninghe Damsté J. S. (2008) Intact membrane lipids of "Candidatus Nitrosopumilus maritimus", a cultivated representative of the cosmopolitan mesophilic group I Crenarchaeota. *Appl. Environ. Microbiol.* 74, 2433–2440.
- Schouten S., Hopmans E. C., Schefuß E. and Sinninghe Damsté J. S. (2002) Distributional variations in marine crenarchaeotal membrane lipids: a new tool for reconstructing ancient sea water temperatures? *Earth Planet. Sci. Lett.* 204, 265–274.
- Schouten S., Hopmans E. C. and Sinninghe Damsté J. S. (2013) The organic geochemistry of glycerol dialkyl glycerol tetraether lipids: A review. *Org. Geochem.* 54, 19–61.
- Schouten S., Villanueva L., Hopmans E. C., van der Meer M. T. J. and Sinninghe Damsté J. S. (2014) Are Marine Group II

- Euryarchaeota significant contributors to tetraether lipids in the ocean? *PNAS* 111, E4285–E4285.
- Sessions A. L., Sylva S. P. and Hayes J. M. (2005) Moving-wire device for carbon isotopic analyses of nanogram quantities of nonvolatile organic carbon. *Anal. Chem.* 77, 6519–6527.
- Seyler L. M., McGuinness L. R., Gilbert J. A., Biddle J. F., Gong D. and Kerkhof L. J. (2018) Discerning autotrophy, mixotrophy and heterotrophy in marine TACK archaea from the North Atlantic. FEMS Microbiol. Ecol. 94, fiy014–fiy014.
- Shah S. R. and Pearson A. (2007) Ultra-microscale (5–25 μg C) analysis of individual lipids by ¹⁴C AMS: assessment and correction for sample processing blanks. *Radiocarbon* **49**, 69–82
- Teira E., Reinthaler T., Pernthaler A., Pernthaler J. and Herndl G. J. (2004) Combining catalyzed reporter deposition-fluorescence in situ hybridization and microautoradiography to detect substrate utilization by bacteria and Archaea in the deep ocean. *Appl. Environ. Microbiol.* 70, 4411–4414.
- Tierney J. E. and Tingley M. P. (2015) A TEX₈₆ surface sediment database and extended Bayesian calibration. Sci. Data 2, 150029, 150029–150029.
- Tolar B. B., Wallsgrove N. J., Popp B. N. and Hollibaugh J. T. (2017) Oxidation of urea-derived nitrogen by thaumarchaeotadominated marine nitrifying communities. *Environ. Microbiol.* 19, 4838–4850.

- Tourna M., Stieglmeier M., Spang A., Könneke M., Schintlmeister A., Urich T., Engel M., Schloter M., Wagner M., Richter A. and Schleper C. (2011) Nitrososphaera viennensis, an ammonia oxidizing archaeon from soil. *PNAS* 108, 8420–8425.
- Weiss R. F. (1970) The solubility of nitrogen, oxygen and argon in water and seawater. *Deep Sea Res. Oceanogr. Abstr.* 17, 721–735.
- Witkowski C. R., Weijers J. W. H., Blais B., Schouten S. and Sinninghe Damsté J. S. (2018) Molecular fossils from phytoplankton reveal secular PCO₂ trend over the Phanerozoic. Sci. Adv. 4, eaat4556.
- Zeebe R. E. (2014) Kinetic fractionation of carbon and oxygen isotopes during hydration of carbon dioxide. *Geochim. Cos*mochim. Acta 139, 540–552.
- Zeebe R. E. and Wolf-Gladrow D. (2001) CO2 in Seawater: Equilibrium, Kinetics. Isotopes. Elsevier Science B.V, Amsterdam.
- Zhang C. L., Xie W., Martin-Cuadrado A.-B. and Rodriguez-Valera F. (2015) Marine Group II Archaea, potentially important players in the global ocean carbon cycle. *Front. Microbiol.* 6, 1108.

Associate editor: Josef P. Werne